

CFD Investigation of Combustion in 660MW Tangential Fired Boiler

Mr. Ashish Fande,

PG SCHOLAR,

Department of Mechanical Engineering

S.S.C.E.T., BHILAI

CHHATISGARH, India

Mr. P. V. Joshi,

Professor,

Department of Mechanical Engineering

S.S.C.E.T., BHILAI

Mr. Sachin Gabhane

Assist. Manager At Adani Power Plant.

TIRORA.INDIA.

Mr. Mukesh Kumar Sahu

Department of Mechanical Engineering

S.S.C.E.T., BHILAI

CHHATISGARH, India

Abstract

Studies into the effects of operating conditions in a tangential fired furnace using commercial code FLUENT is explained in this paper. A 3-D combustor model is used to determine the temperature, velocity and other thermal characteristics like O_2 mass fraction, CO_2 mass fraction for a typical 660 MW utility boiler firing medium volatile coal. Particle trajectories are studied to identify the causes of operational problems such as fouling on burners, and temperatures achieved in various parts of the boiler during the combustion process. In this project peripheral air concentric to the primary air with coal in the furnace temperature pattern is considered. For these we have done a numerical study of flow of reactive gas mixture with pulverized coal combustion occurring in tangential fired furnace. Study Model calculations showed good agreement with experimental measurements plant data. The experience obtained Using these CFD model studies can improve the operation of a boiler by varying its flow parameter inside the boiler, which built a foundation for the boiler operating expert system.

Keywords: tangential fired furnace, Grid generation, CFD, Turbulent flow, Multiphase flow, Particle trajectories, temperature in various zones of boiler, species like O_2 & CO_2 distribution.

1. Introduction

In recent years the interest on performance optimisation of large utility boilers has become very relevant. All the optimisation thinking are directed at extending their lifetime, for increasing the thermal efficiency and reducing the pollutant emissions from combustion. Moreover, efficient use of pulverised coal is crucial to the utility industry. To get higher combustion efficiency, the major influencing factors such as the particle size distribution, gas and particle temperatures, local heat release, local oxygen concentration, kinetic parameters for coal de-volatilization and char oxidation, char properties should be understood thoroughly [1,2]. In an engineering practice, it is very difficult to study the combustion processes of various kinds of combustibles directly in the boiler than constructing real boilers and trying to these characteristics, computers are used to experiment with models of the boilers.

One of the techniques to visualise parametric effects in boilers is computational fluid dynamics (CFD) modelling, which potentially can be an accurate and cost effective tool. Over the last 20 years, the CFD has gained its reputation of being an effective tool in identifying and solving problems related to pulverized coal combustion [3–4]. In particular, it can provide insights into the combustion characteristics of unfamiliar coals and for this reason has been extensively applied to evaluate the combustion performance of coals in bench-, pilot-and full-scale furnaces.

In the present study, an attempt has been made to simulate and visualise the furnace operation, based on parameters of interest to the combustion process through CFD modelling. These parameters include temperatures achieved in various parts of the boiler, particle residence time, particle velocity, O_2 and CO_2 distribution within the furnace. This paper concentrates on the prediction of furnace performance for different boiler operating conditions. The boiler geometry and operating conditions along with the mathematical model used are detailed in the following section. Results simulated are based on real cases (different operating conditions used in the industry), but the data sources have necessarily been disguised to the extent that industry proprietary concerns are not infringed. It must be mentioned that the verification of the computational simulations are expensive to obtain, but even if the user has experimental data available, the comparison between these data and predictions leaves the user uncertain about both the errors in the model and experimental data. Nevertheless, using the experience obtained by a CFD model can significantly improve the operation of a boiler, regarding stability and local material temperature of boiler.

2. Furnace geometry and operating conditions

The boiler geometry is to be constructed in such a way that depending upon its dimension as height, length and depth from ground. The width of the furnace is 19824mm, while the depth is 17640mm. Elevation of the water wall lower header is 9000mm; elevation of centerline of roof is 77800mm, and elevation of the main girder bottom is 85700mm. Thirty two burners are arranged in the corner of boiler. Total 8 mills are located for coal with primary air firing each mill having four burners and the mill are spaced at the certain distance as 972.4 mm. with each other. In between mill there is some provision for firing secondary air. Boiler combustion system is design according to medium speed pulverizers and cold primary air direct-fired system. 32 direct air burners are arranged at the lower four corners of the furnace in 8 layers, and power coal and air are loaded through the four corners to burn in the furnace tangentially. The Nozzle center elevation of the top row of burner is 39780mm and is 20020mm far from the platen bottom. The Nozzle center elevation of the bottom row of burner is 26150mm and is 5131mm far from the furnace hopper corner. Technology, quick ignition pulverized coal nozzle etc. burners in the corners. The velocity of coal+air is shown in table 1[9].

On upper part of the furnace platen superheater and high temperature superheater are arranged. Platen superheater, high temperature superheater and reheater are fixed by fluid cooled spacer tube along the furnace width direction. A fluid cooled spacer tube is led out from the backpass extending side wall lower header, converging with the main pipe before entering the secondary desuperheater. Superheater steam temperature is controlled by coal-water ratio adjustment and two-stage spray water. The primary desuperheater is located at the low temperature superheater outlet piping, while the secondary one is at the platen Geometry and distribution of inlet sections along the height of each corner of the furnace Superheating and two reheating sections are located. Economizers are located in the rear pass of combustion gases. The coal used in this boiler based on the proximate and ultimate analysis shown in table 2[9]. The complete set of three dimensional arrangement of boiler and side view of tangential fired boiler is shown in fig. 1.

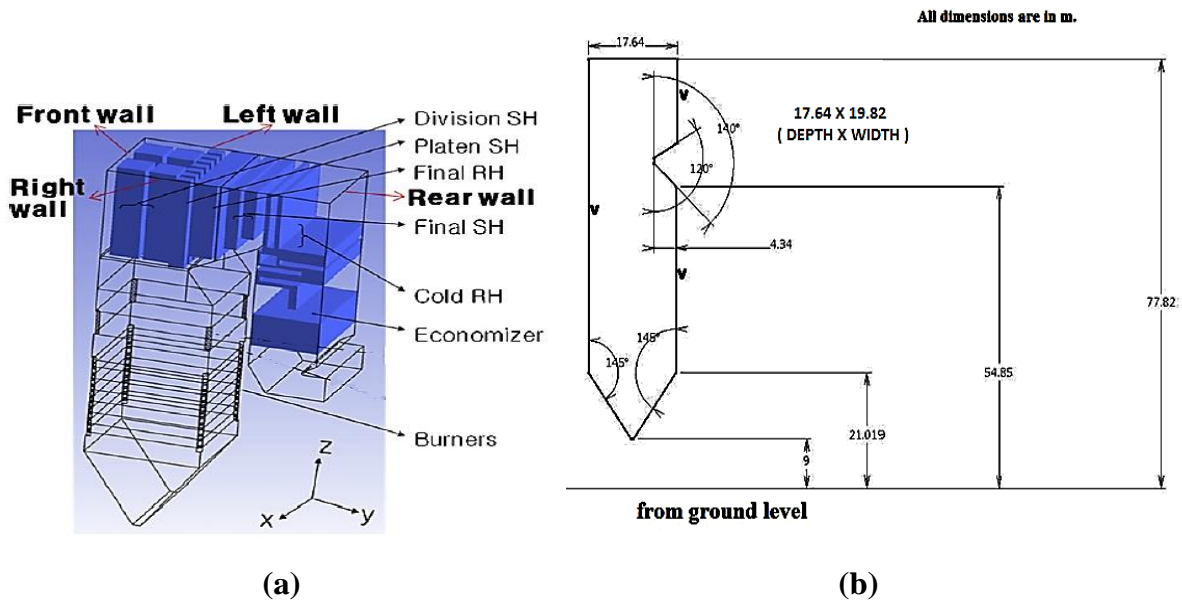


Fig. 1 (a) Three dimensional arrangement of boiler (b) side view of tangential fired boiler

Fig.2. shows in detail the arrangement of air and coal nozzles. Different inlet sections are represented, corresponding to the mixture of primary air and pulverized-coal (PA + PC), the secondary air (SA) and also the fuel-oil used during start-up (FO). Surrounding the primary air and pulverized-coal entrance, a narrow square ring also introduces a small flow of peripheral secondary air. Different orientations can be imposed for the entering streams, separately for primary air + pulverized-coal and for secondary air.

The boiler furnace geometry of the simulated boiler can be seen in Fig. 3. The 3dimensional geometry is created using Ansys workbench software. The meshed-geometry contained 1,72,640 nodes with tetrahedral cells throughout the geometry .In order to make correct quantitative predictions about ignition behavior, it is necessary that an appropriate geometry is created with convenient meshing techniques. A more refined mesh is provided near the burner and air inlet. About 50% to 60% of the project time is involved in creating the model geometry. Primary and secondary air inlet details are taken according to the actual burner dimensions. The swirl angle is not considered for the present study.

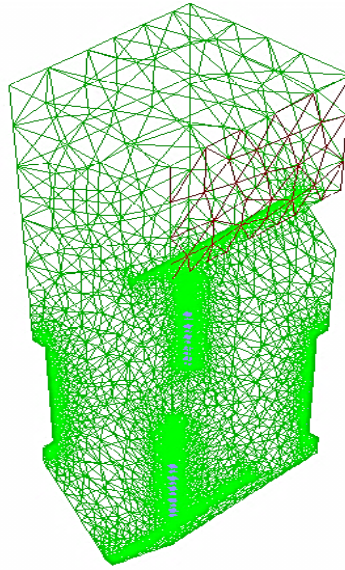


Fig.3. Grided geometry of boiler

Operating condition for CFD simulation

Table 2. Main boiler operating conditions in boiler[9].

Case description	1 st Mill (In Each Burner)	2 nd Mill(In Each Burner)	3rd Mill(In Each Burner)	4rth Mill (In Each Burner)	5th Mill(In Each Burner)
P.A. velocity(m/s) & temperature (K)	24.6m/sec &343k	24.6m/sec &343k	24.6m/sec &343k	24.6m/sec &343k	24.6m/sec &343k
S.A velocity(m/s) & temperature (k)	37m/sec & 598k	37m/sec & 598k	37m/sec & 598k	37m/sec & 598k	37m/sec & 598k
P.S.A velocity(m/s) & temperature(K)	19 m/sec &598k	19 m/sec &598k	19 m/sec &598k	19 m/sec &598k	19 m/sec &598k
Total coal feed rate (kg/s)	3.47	3.47	3.47	3.47	3.47
Calorific value	1.64e ⁺⁰⁷	1.64e ⁺⁰⁷	1.64e ⁺⁰⁷	1.64e ⁺⁰⁷	1.64e ⁺⁰⁷

WHERE,

P.A.For Primary Air Velocity.

S.A. For Secondary Air Velocity.

P.S.A.For Peripheral Secondary Air Velocity.

Table 3. Proximate and ultimate analysis of the coal-fired during the tests[9].

Proximate analysis	(% db)	Ultimate analysis	(% daf)
Moisture	17	Carbon	74.42
Ash content	4	Hydrogen	4.9
Volatile matter	37	Nitrogen	1.5
Fixed carbon	43	Sulfur	1.0
Total sulphure	0.83	Oxygen	18.13

3. Mathematical model

The mathematical model implemented here is totally based on the commercial CFD code, FLUENT, where the gas flow is described by the time averaged equations of global mass, momentum, enthalpy and species mass fraction. The equations, which are elliptic and three-dimensional, were solved to provide predictions of the flow pattern, thermal and pollution characteristics of reacting flows inside a model of an industrial boiler. Operating parameters include the air to fuel ratio, combustion air temperature and swirl angle. The governing equations, turbulence model, the boundary conditions and the solution procedure are presented in the following sections.

$$\frac{\partial}{\partial x_j} (\bar{\rho} \bar{u}_j \phi + \bar{\rho} \bar{u}_j \phi) = \frac{\partial}{\partial x_j} \left[\Gamma_\phi \frac{\partial \phi}{\partial x_j} \right] + \bar{\rho} S_\phi \quad (1)$$

Where, ϕ is the dependent variable and u_j is the velocity component along the coordinate direction x_j . $\bar{\rho}$ is the fluid density; Γ_ϕ is the diffusion coefficient and S_ϕ is the source term. Eq. (1) stands for the mass conservation equation when $\phi = 1$; the momentum conservation equation when ϕ is a velocity component; the energy equation when ϕ is the stagnation enthalpy; or the transport equation of a scalar when ϕ is a scalar variable such as mixture fraction.

The standard k- ϵ turbulence model, single mixture fraction probability density function (PDF) and the P1 radiation models are used in the present simulations. For the bulk of engineering combustion systems the mixing process proceeds much more slowly than the chemistry and as a result the mixing rate almost always determines the rate of combustion [6].

Therefore, for the predominant industry case of 'diffusion' or non-premixed combustion for example, it normally suffices to solve a conservation equation for a mixing variable called the 'mixture fraction' in order to determine the temperature and concentrations of major species. In this study, a simplified coal combustion furnace is modeled using the non-premixed combustion model for the reaction chemistry. The following steps describe the method followed, after creating the required geometry.

- 1) A PDF table for a pulverized coal fuel using the PDFPre-processor has been prepared for medium volatile coal.
- 2) FLUENT inputs for non-premixed combustion chemistry modeling were estimated.
- 3) A discrete second phase of coal particles was defined.
- 4) Simulations which were carried out first without involving reactive mixture and discrete coal particles and then once the solution convergence is achieved, furthermore simulations were continued involving reacting discrete phase coal particles. The composition in terms of atom fraction of H, C, N, O, S along with the lower heat value and heat capacity of the fuel are defined using the data provided by a 660MW power plant. The volatile release model is based on a single kinetic rate model [7,8]. This model states that the production rate of volatile gases is given by a first order reaction, which correlates rates of weight loss with the temperature.

As in most practical fossil-fuel combustion simulations, the incompressible form of the equations of motion using a finite volume form of the discretization equations are solved with SIMPLE-based approaches. It is also assumed that the flow field is at a steady-state and the solution procedure is simplified by solving a steady-state form of the equation of motion. For many combustion processes, radiation is not only the dominant energy transport mechanism but also one of the most complex problems. The accuracy of the radiation calculation depends on a combination of the accuracy of calculation method and the accuracy to which the properties of the radiating media and surrounding walls are known [4]. The P1 radiation model is used to account for the exchange of radiation in furnace, which specifies a composition dependent absorption coefficient. All thermodynamic data including density, specific heat, and formation of enthalpies are extracted from the pre-PDF chemical database.

4. Results and discussion

The computational model has been applied to the furnace of 660 MW boiler fired with high-ash, medium volatile coal. The input data for CFD simulations (including boiler

operational conditions) is selected in correspondence with data related to the experimental tests of the considered boiler. The properties and the lower heating value of fuel mass “as received” basis at a local power station are assumed in calculations. The yield of volatile matter was taken according to the data provided. Although, the full-scale boiler is equipped with 32 conventional burners having eight mills of the swirling type arranged on each corner, here only five mills are considered as full load (hereafter referred to as base case) for modelling the operation.

At first, only the gas flow equations are solved in order to achieve for stable calculations and fast convergences for two-phase flow, combustion, heat-transfer and chemical reactions. After the flow field converges, the trajectories of the coal particles interacting with the flue gas are calculated. Next, the chemical reaction and enthalpy equations for coal combustion are taken into account. Numerical calculations are repeated until the flow and temperature converge. A convergence criterion is that the normalized residuals for all the variables need to be less than 10^{-3} . Flow and temperature field convergence is obtained after more than 1465 iterations. Scaled residuals for total combustion process including the discrete phase is shown in fig 4.

The predicted temperatures at the furnace exit are 1545K, while the measured temperatures are 1600K. The predicted molar fraction of O₂(%) and CO₂(%) at the boiler furnace exit are 0.7% and 16% respectively.

Table 3. Comparison of predicted outlet temperatures with measurements in experimental data.

	Section name	Plant measurement	Predicted measurement
Temperature[K]	Furnace exit	1600	1545
O ₂ [% ,molefraction]	Furnace exit	-	0.7%
CO ₂ [% , mole fraction]	Furnace exit	12 %	16 %

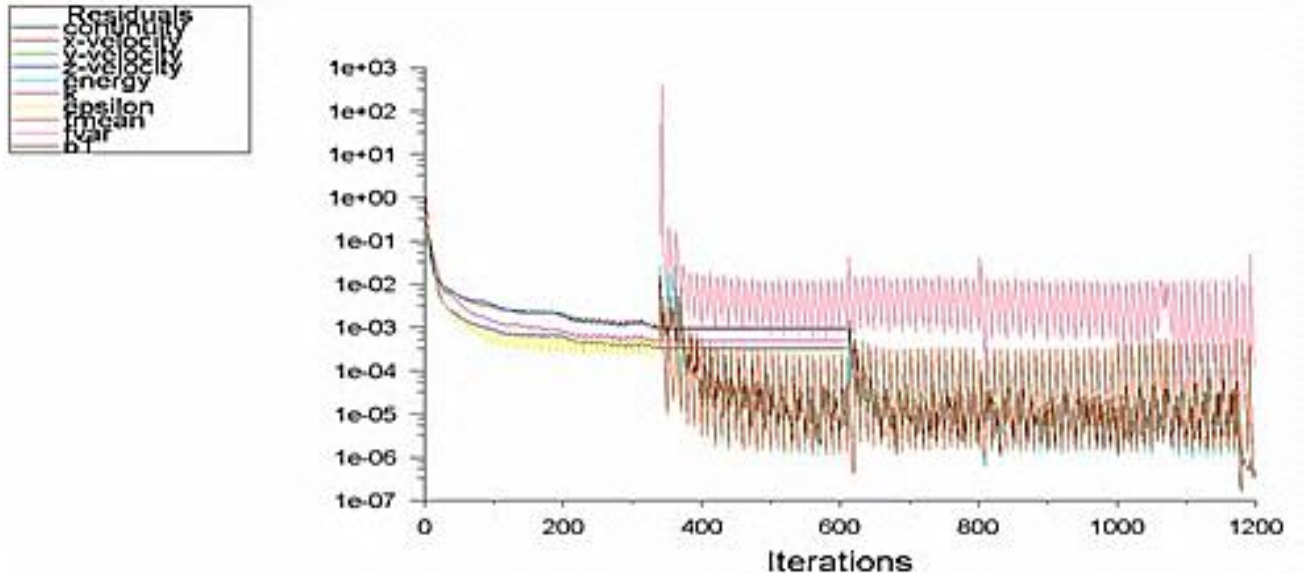


Fig.4.Scaled residualsfortotalcombustionprocessincludingthediscretephase.

4.1Flow fields and coal particle trajectories

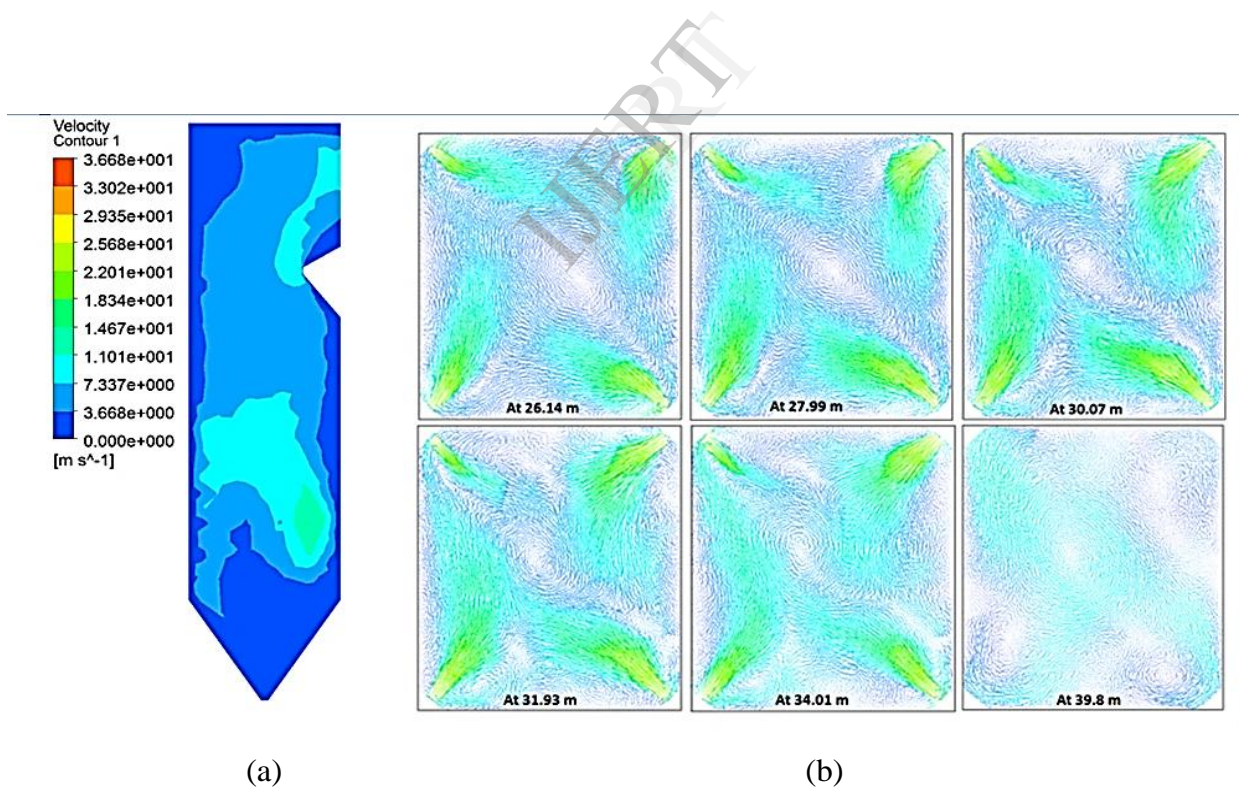


Fig.5.Flow fields of coal +airinlet (a) velocity magnitude(b) velocity vector

The velocity distribution and vectors in cross sections along the furnace height are shown in Fig.5. The flows located near the burners show more activity than in other locations. A clockwise swirling flow formed via the air and coal particles injected through the burner ports is

found in the center of the furnace, as expected. The swirling flow is stronger in the lower level at 26.14 m from ground level than in the higher level at 30.07 m. In the upper region (at 34.01m & 39.8m), the swirling flow is remarkably reduced. The flue gas flows into the primary super-heater with a mean velocity of 8.01 m/s and standard deviation of 3.32m/s. The upward velocity distribution located downstream above the burner's inlet is relatively flat and the swirling flow is very weak. This implies that the equipment like super-heaters and re-heaters installed downstream help the flow to be even and the residual swirling flow to be reduced.

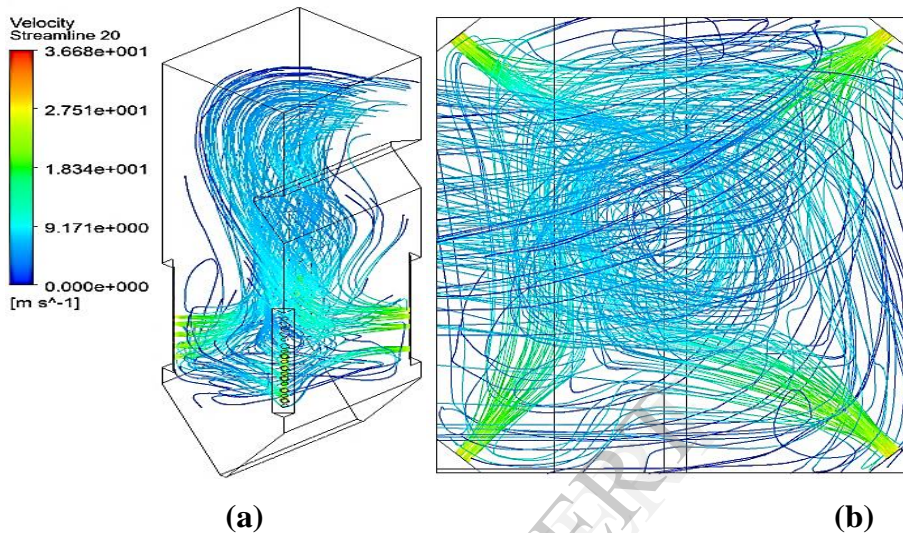


Fig.6. Streamline of the flue gas and coal particle (a) isometric view (b) top view

The streamlines of the flue gas and the trajectories of the coal particles are depicted in Fig.6. The streamlines and trajectories show very complicated three-dimensional flow characteristics which promote the mixing of the air and coal particles and enhancing heat transfer via bulk motion. The coal particle trajectories are very similar to the flue gas path lines but not coincident due to the different densities and turbulent fluctuations. The flue gas and coal particles injected from the lower burners, initially circulate in the bottom of the furnace and the ash hopper and eventually travel up through the high-temperature and swirling-flow region (so-called fire-ball) formed in the central region of the furnace, while the flue gas and coal particles from the higher burners pass around the surface of the fire-ball region. As a result, the residence times of the flue gas, and coal particles injected from the higher burners are shorter in comparison to the flue gas and coal particles injected from the lower burners. The average residence time and traveling length of the flue gas within the boiler are 22.2 s and 162 m, respectively, and these values are listed in Table 4.

Table 4 Summary of flue gas behavior

Flue gas	Avg. Residence time [s]	22.2
	Traveling length [m]	162 m

Coal devolatilization and char combustion take place while the coal particles are traveling around the furnace, as shown in Fig. 6. Moreover, residence time and turbulence are always considered together: the more turbulence inside furnace, the longer the residence time of the coal particles. It is obvious that the residence time depended strongly on the height of the burner; the residence time decreased with increasing height of burner positions. In general, it is known that all fuel species except char are consumed very quickly in the furnace. However, char burns at a slower rate and is consumed in the central region of the furnace. In this calculation, the conversion ratio of the combusting particles is approximately 100%. This implies that the present combustion processes offer sufficient residence time even for char conversion.

4.2. Temperature distributions

The temperature distributions in the cross sections are shown in Fig. 7. The temperature of the flue gas is relatively high in the central region of the furnace where coal combustion actively takes place. The change pattern of the flue gas temperature is clearly shown along the furnace height in Fig. 7b. The temperature of the air injected from the burners corner is 343 K, and it increases up to a maximum temperature of 1800 K in the central region of the furnace. A noticeable temperature deviation is seen in the lower level of the furnace, but in the higher levels, the temperature deviation decreases due to stronger swirling and increased mixing. Along with the increased height, the average temperatures in each cross sections also increase because of high combustion intensity. However, as the flue gas goes upward in the furnace, the temperature of the flue gas decreases due to the heat transfer between the flue gas and furnace walls via convection and radiation. Finally, the flue gas leaves the boiler furnace at an average temperature of 1,545 K. The iso-surfaces at temperatures of 1800 K indicating high temperature zones in the furnace are depicted in Fig. 10a. These high temperature regions are closely related to NO_x formation which is dependent on local temperature.

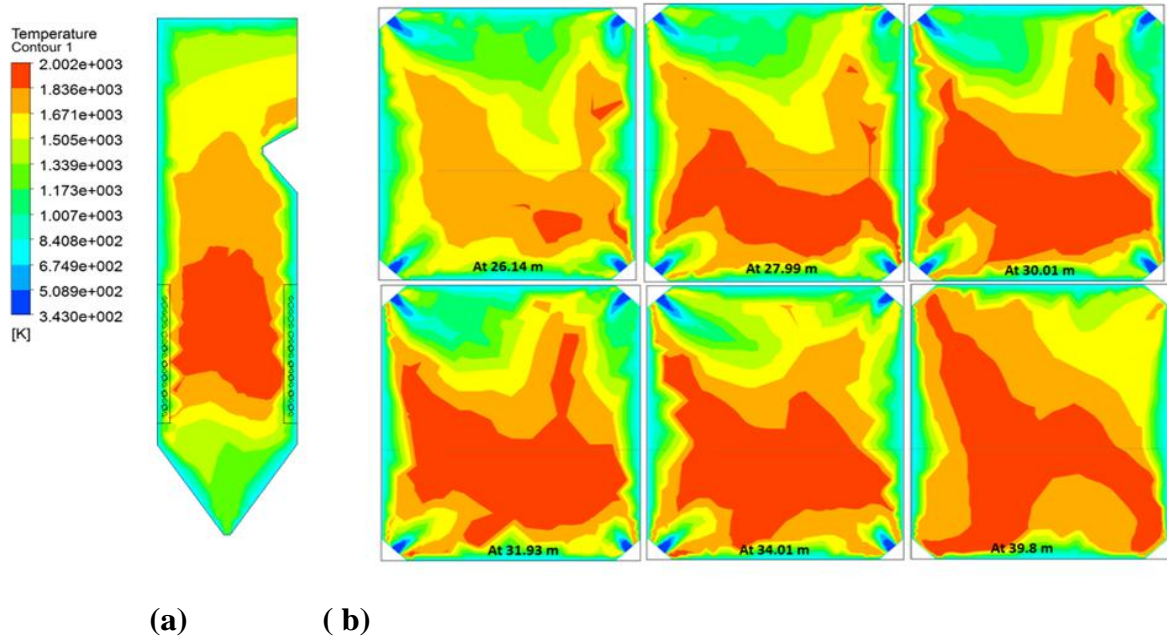


Fig.7. Temperature fields in a coal fired furnace (a) along vertical section (b) along horizontal section.

4.3 O₂ distributions

The mass fraction distributions of O₂ are depicted in Fig. 8.

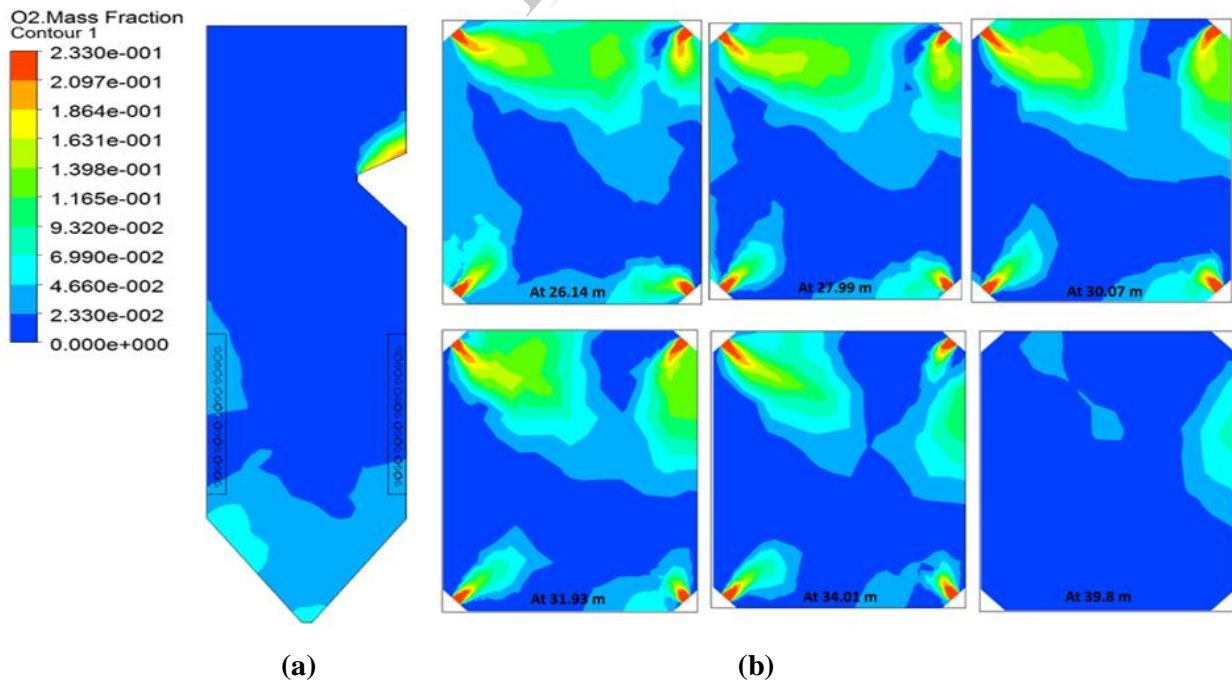


Fig.8 O₂ distribution in tangential fired boiler (a) along vertical section (b) along horizontal section.

The O₂ concentration in the furnace is relatively higher near the burners. The O₂ contained in the air injected inside the furnace, where the temperature is relatively higher, is quickly consumed during the combustion processes. Due to which, the O₂ mass fraction rapidly decreases. In particular, the O₂ mass fraction remarkably decreases near the burners, where combustion is more and more active, and the fuel volatile species are more rapidly consumed. As depicted in Fig. 7, the high temperature regions in the furnace roughly correspond to the regions of the lower O₂ mass fraction. The iso-surfaces at O₂ of 4.5% indicating high oxygen containing zones in the furnace are depicted in Fig. 10b. These high oxygen regions are closely related to increasing the temperature inside boiler and proper combustion of fuel.

4.4 CO₂ distributions

The CO₂ distributions in the cross sections are shown in Fig. 9.

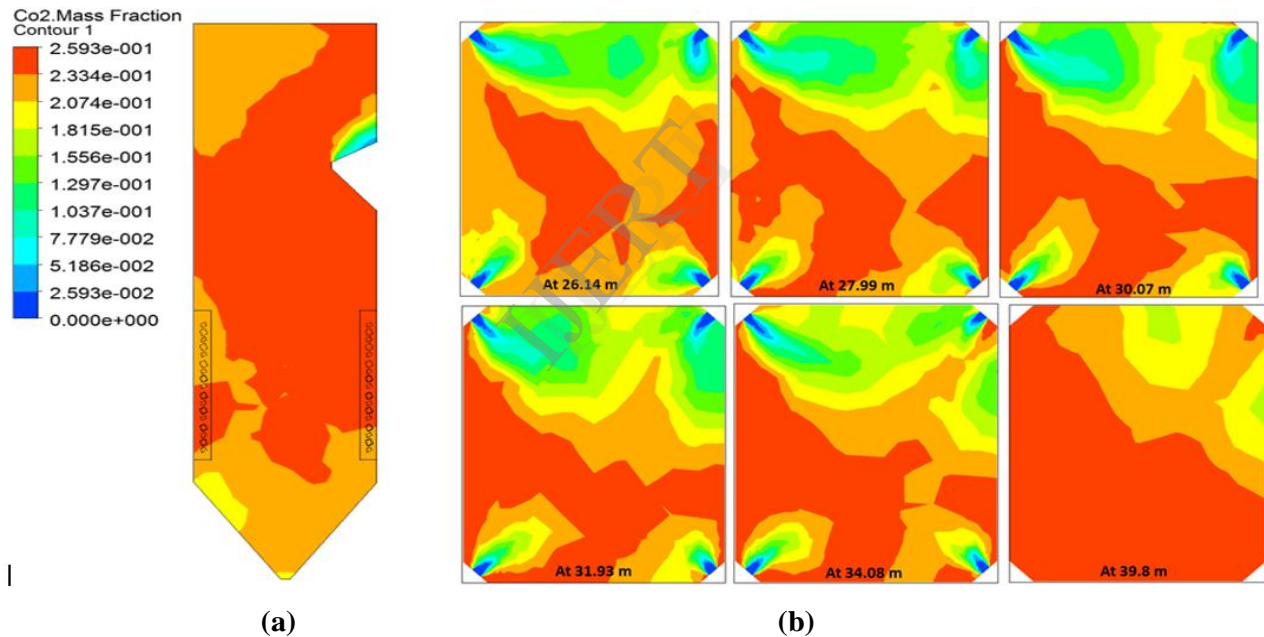


Fig. 9 CO₂ distribution in tangential fired boiler (a) along vertical section (b) along horizontal section

In contrast to the O₂ mass fraction, the CO₂ mass fraction significantly increases as the air moves from the burners due to the active combustion processes. High peaks of the O₂ mass fraction are shown in the middle zone of the furnace when the CO₂ mass fraction is low, which suggests that the sudden variation in their values is due to the supply of combustion air through the burners. In Fig. 7b, as the temperature of the flue gas increases, the O₂ mass fraction decreases steeply while the CO₂ mass fraction increases because volatile combustible contents of the coal burn near the burners.

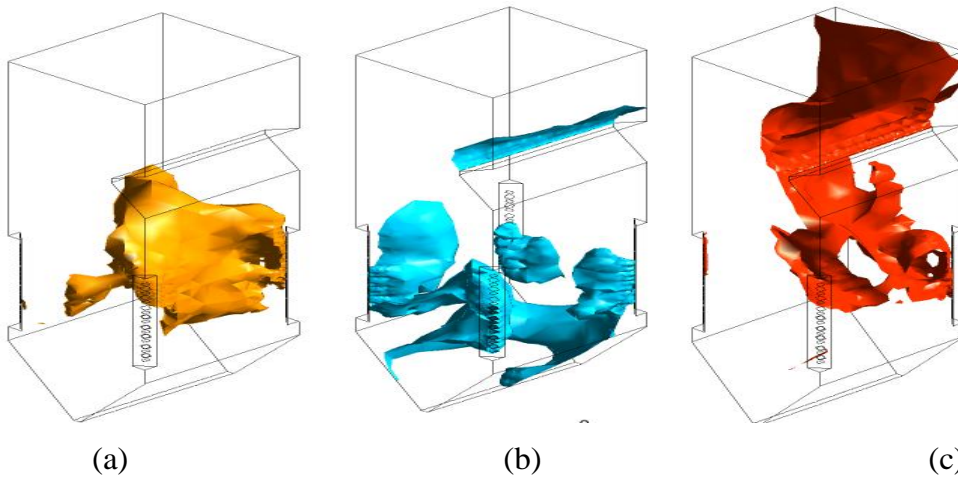


Fig.10.(a) iso-surface indicating high temperature zone (1800k) (b)) iso-surface indicating high O₂ mass fraction (4.5%) (c)) iso-surface indicating high CO₂ mass fraction (24%).

The iso-surfaces at CO₂ of 25% indicating high CO₂ containing zones in the furnace are depicted in Fig. 10c. These high CO₂ regions are closely related to decreasing the oxygen mass fraction inside boiler.

The variation of species concentration and temperature along the furnace is shown in figure 11.

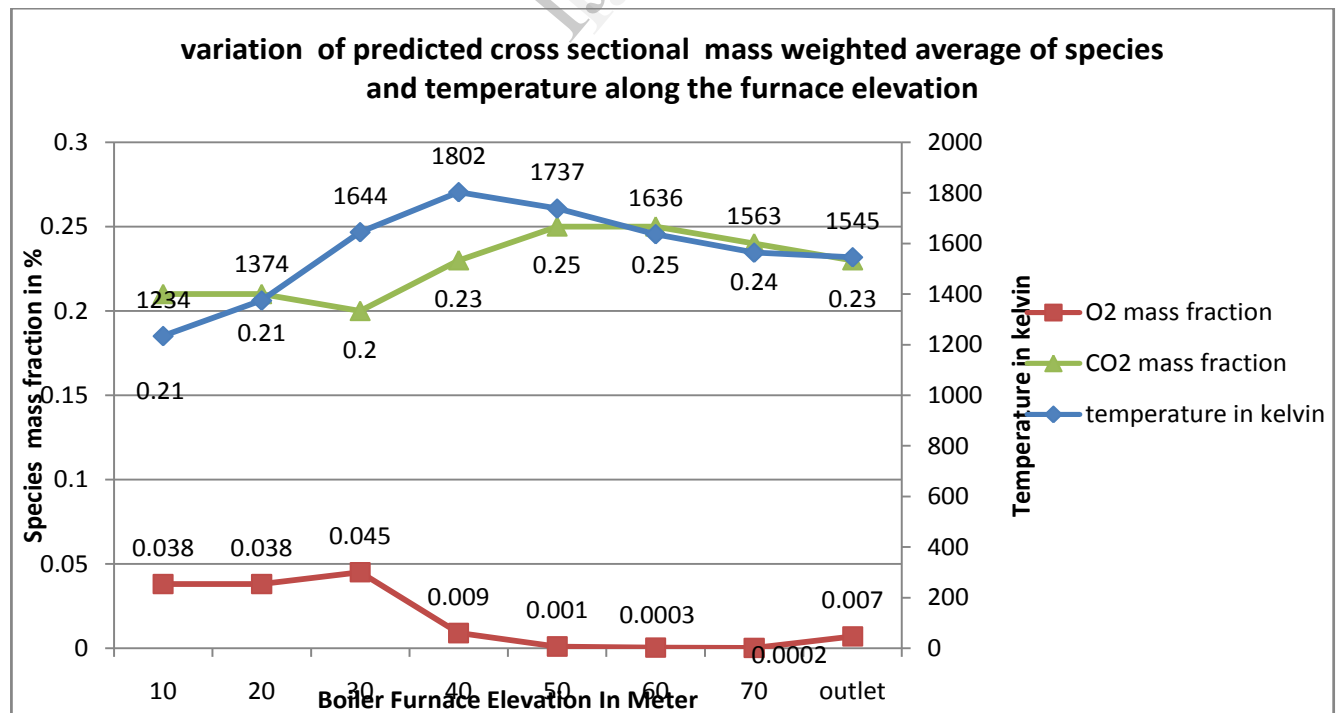


Fig.11. variation of species concentration and temperature along the furnace

5. Conclusions

Modelling of a tangential fired furnace is carried out using CFD commercial flow solver FLUENT. Simulation results with different burners in operation suggested a significant impact on the distribution of temperatures and furnace exit temperatures. This indicates that extreme care must be taken in terms of maintenance and service of burners so as to minimize the effects on combustion and continue smooth operation of boilers. Predicted particle trajectories indicate differences in particle residence times within the boiler. In particular, particles emerging out lower burner sections tend to reside within the boiler longer than the particles at other locations. This may lead to poor combustion, which is undesirable for efficient operation of power station boilers. The simulation of this boiler using fluent we visualise what will be temperature in various zones of boiler. The relation among the temperature, O₂ mass fraction and CO₂ mass fraction has been clearly demonstrated based on the calculated distributions. Overall the model results showed good agreement with measured and reported data, which provides a solid foundation for future work. Data presented in the paper demonstrates the implications and possible options for burner operations in terms of their maintenance and serviceability. The results obtained with such models would prove to be of practical value to optimize the performance of boilers.

References

- [1] Minghou Xu, J.L.T. Azevedo, M.G. Carvalho, Modeling of a front wall fired utility boiler for different operating conditions, *Comput. Methods Appl. Mech. Eng.* 190 (2001) 3581–3590.
- [2] S. Chapman, T.G. Cowling, *The Mathematical Theory of Non-Uniform Gases*, Cambridge University Press, Cambridge, UK, 1990.
- [3] S. Niksa, *Coal Combustion Modelling*, IEAPER/31, IEA Coal Research, London, 1996.
- [4] M. Eaton, L.D. Smoot, S.C. Hill, C.N. Eatough, Components, formulations, solutions, evaluation, and application of comprehensive combustion models, *Prog. Energy Combust. Sci.* 25 (1999) 387–436.
- [5] T. Abbas, P.G. Costen, F.C. Lockwood, *26th Symposium (International) on Combustion*, The Combustion Institute, 1996, p. 3041.
- [6] P.G. Costen, D. Dajnak, M. Messina, F.C. Lockwood, T. Abbas, C. Bertrand, N.H. Kandamby, V. Sakthitharan, I. Siera, S. Yousif, On the prediction and control of industrial combustors by mathematical modelling, Paper presented at 2002 Australian Symposium on

Combustion and The Seventh Australian Flame Days, Adelaide, February 2002.

[7] FLUENT, FLUENT 6.2 Users Guide, 2005 Lebanon, USA.

[8] Williams, R. Backreedy, R. Habib, J.M. Jones, M. Pourkashanian, Modelling coal combustion: the current position, Fuel 81 (2002) 605–618.

[9]Shangai boiler works limited user manual.

IJERT